Volume 16
Number 8
28 February 2025
Pages 917-1012

Polymer Chemistry

rsc.li/polymers

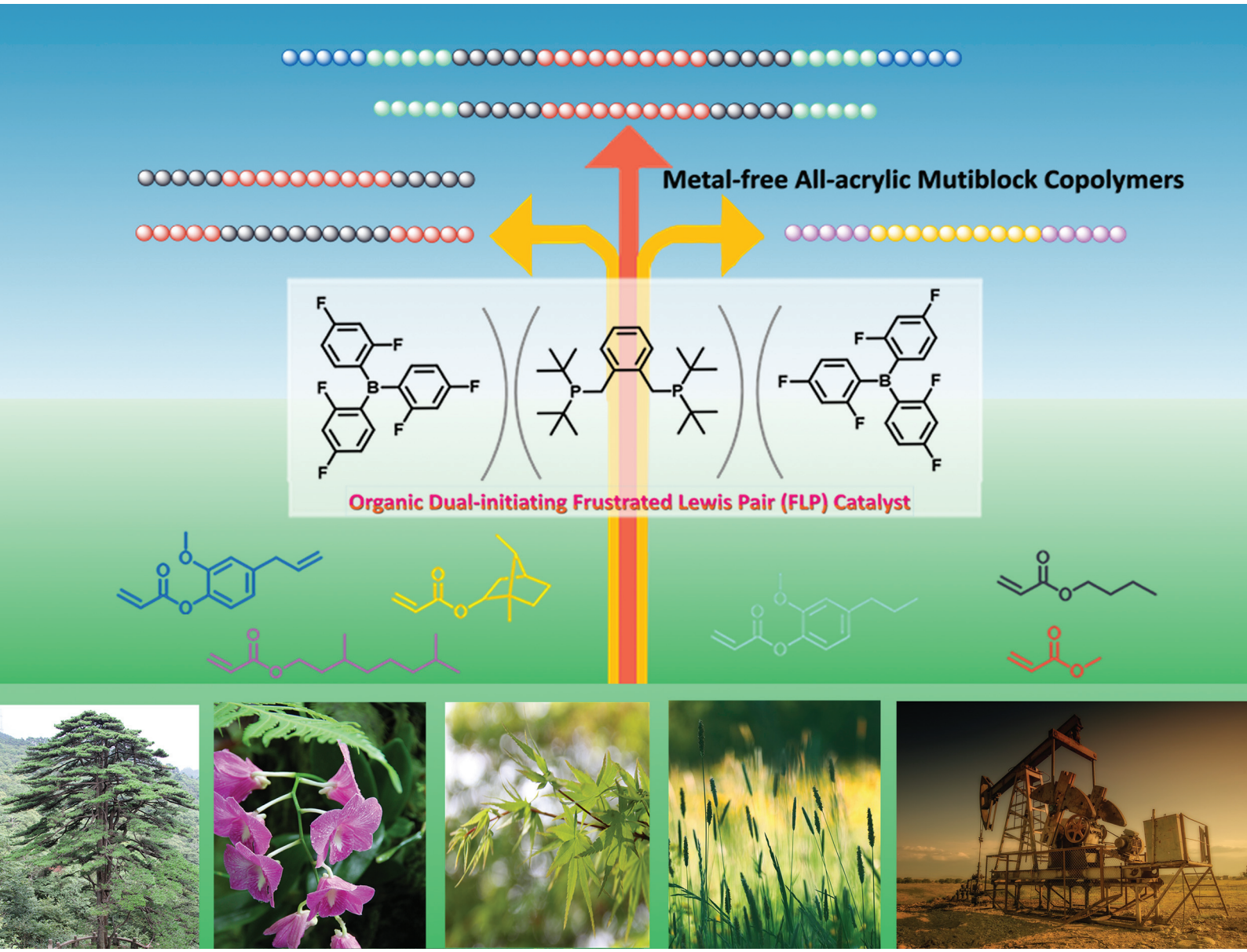

ISSN 1759-9962

ROYAL SOCIETY OF CHEMISTRY

PAPER
Miao Hong *et al.*
A dual-initiating organic frustrated Lewis pair catalyst for living polymerizations of (bio)acrylates to facilitate the synthesis of metal-free multiblock copolymers

15 YEARS ANNIVERSARY

Polymer Chemistry

ROYAL SOCIETY OF CHEMISTRY

PAPER

View Article Online
View Journal | View Issue

Cite this: *Polym. Chem.*, 2025, **16**, 936

A dual-initiating organic frustrated Lewis pair catalyst for living polymerizations of (bio)acrylates to facilitate the synthesis of metal-free multiblock copolymers†

Zhen-Hua Zhang,‡[a,b] Yuyang Chen,‡[b] Yuesheng Li [a] and Miao Hong *[b,c]

Received 24th September 2024,
Accepted 16th December 2024

DOI: 10.1039/d4py01067a

rsc.li/polymers

The development of powerful catalysis or methodologies for the synthesis of fundamentally and technologically important multiblock copolymers is a perpetual task. Dual-initiating Lewis pair (LP) catalysts for living/controlled polymerizations of methacrylates have been demonstrated to be an effective approach towards all-acrylic multiblock copolymers. However, the utilization of metal-based Lewis acids (LAs) and complicated Lewis bases (LBs) that typically require laborious syntheses are essential. This article reports the first organic dual-initiating frustrated Lewis pair (FLP) catalysts consisting of tris(2,4-difluorophenyl) borane [B(2,4-$F_2C_6H_3)_3$] LA and commercially available 1,2-bis[(di-*tert*-butylphosphino)methyl]benzene (DP^tBu_2) LB, which can mediate efficient and living polymerizations of various (bio)acrylates. Accordingly, all-acrylic multiblock copolymers (up to hepta blocks) with well-defined structures can be readily prepared *via* sequential monomer addition, thus successfully establishing DP^tBu_2/B(2,4-$F_2C_6H_3)_3$ FLP as a green/sustainable and user-friendly polymerization catalyst for the convenient synthesis of metal-free all-acrylic multiblock copolymers.

Introduction

Lewis pair polymerization (LPP) is a newly emerging polymerization methodology which is catalyzed by a frustrated Lewis pair (FLP) or a classical Lewis adduct (CLA) that can dissociate into an FLP in the presence of a suitable solvent or monomer.[1–5] Inspired by FLP chemistry for cooperative activation of small molecules,[6,7] Chen and coworkers reported the first LPP in 2010 through uncovering highly efficient polymerization of methyl methacrylate (MMA) and γ-methyl-α-methylene-γ-butyrolactone (MMBL) by a Lewis pair (LP) catalyst consisting of $Al(C_6F_5)_3$ Lewis acid (LA) and P^tBu_3 or N-heterocyclic carbene Lewis base (LB).[8]

Subsequently, the contributions from the groups of Chen,[8–15] Zhang,[16–27] Lu,[28–30] Xu,[31–35] Hong,[36–41] Zhu,[42,43] Rieger,[44,45] Takasu,[46,47] and Matsuoka[48–51] *etc.* have demonstrated LPP to be a very powerful methodology which not only enables the efficient and/or living polymerizations of various polar vinyl monomers [*e.g.* methacrylates,[8,16,17,28] acrylates,[39,47,48,50–52] acrylamides,[20,49] vinylpyridine,[10,34] and dialkyl vinylphosphonate[44,45]], but also achieves chemoselective polymerizations of polar divinyl monomers,[21,29–31] regioselective polymerizations of (*E*,*E*)-alkyl sorbates,[19] stereoselective polymerizations of methacrylates,[35,36] and topology-controlled polymerizations (*e.g.* cyclic polymers).[13,14,23,46,47] Moreover, in response to the ever-growing demand for sustainable polymers, the scope of polar vinyl monomers has also been extended to biomass-derived vinyl monomers, such as lignin-based methacrylates,[22,25] methyl crotonate,[15] (*E*,*E*)-alkyl sorbates,[19,46] methylene butyrolactones,[8,9,40,41] and cellulose-derived β-angelica lactone.[37,38] The successes achieved in the field of LPPs are closely related to the unique ability of both unquenched LB and LA sites of LP catalysts to cooperatively activate monomers as well as to stabilize the propagating active species to suppress chain transfer and termination side reactions.[1–5]

On the other hand, the development of powerful catalysis or methodologies for the synthesis of multiblock copolymers is a perpetual fundamental task because these copolymers can lead to the formation of highly ordered materials with unique functions and advanced properties (*e.g.* thermoplastic elasto-

[a]*Tianjin Key Lab of Composite & Functional Materials, School of Materials Science and Engineering, Tianjin University, Tianjin 300072, China*
[b]*State Key Laboratory of Organometallic Chemistry, Shanghai Institute of Organic Chemistry, Chinese Academy of Sciences, Shanghai 200032, China. E-mail: miaohong@sioc.ac.cn*
[c]*School of Chemistry and Materials Sciences, Hangzhou Institute for Advanced Study, University of Chinese Academy of Sciences, 1 Sub-lane Xiangshan, Hangzhou 310024, China*

†Electronic supplementary information (ESI) available. See DOI: https://doi.org/10.1039/d4py01067a

‡These authors contributed equally to this work.

mers (TPEs), nanotechnology *etc.*).[53–55] Recently, the development of dual-initiating LP catalysts for controlled/living polymerizations has been demonstrated to be an efficient approach towards all-acrylic multiblock copolymers. In 2021, Zhang and co-workers developed a new FLP catalyst comprising a sterically encumbered methylaluminum bis(2,6-di-*tert*-butyl-4-methylphenoxide) [$MeAl(BHT)_2$] LA and bifunctional organophosphorus superbase (μ^{Hex}[P(NI^{i}Pr)Ph]$_2$, Scheme 1, top), which established the first dual-initiating and living LPP for the successful preparation of triblock TPEs containing soft midblock poly(2-ethyoxyethyl methacrylate) and hard end block PMMBL.[24] Subsequently, through the integration of the unique compounded sequence control (CSC) strategy of LPP and a dual-initiating FLP catalyst consisting of ^{i}Bu$_2$Al(BHT) LA and pyridinylidenaminophosphine (μ^{Oct}[P(mMPy)Ph$_2$]$_2$, Scheme 1, top), one-step and one-pot block copolymerizations from lignin-based syringyl methacrylate and *n*-butyl acrylate (^{n}BA) monomer mixtures to triblock TPEs[25] as well as from MMA, MMBL, ^{n}BA, and *t*-butyl acrylate (^{t}BA) monomer mixtures to sequence-controlled multiblock copolymers (up to hepta blocks)[26] have been achieved by Zhang *et al*. In 2023, up to undecablock all-acrylic copolymers can be synthesized with a three-step monomer mixture feeding by Zhu, Zhang, and co-workers *via* the development of a new dual-initiating CLA catalyst based on $MeAl(BHT)_2$ LA and bis-phosphonium ylide LB (Scheme 1, top).[43] Very recently, Zhang's group designed novel tetraphenylethylene-linked N-heterocyclic olefins (NHOs) as dual- and tetra-functional LBs (Scheme 1, top). By combining with ^{i}BuAl(BHT)$_2$ LA, the resultant LPs can yield sequence-controlled linear and four-arm star triblock TPEs *via* one-step and one-pot block copolymerizations.[27]

As revealed by above overview, although several dual-initiating LP catalysts have been developed for the synthesis of all-acrylic multiblock copolymers, air/moisture sensitive metal-based LAs and complicated LBs that typically require laborious syntheses are essential.[56–58] Compared with metal-based catalysts, organic catalysts are, in general, relatively non-toxic, environmentally benign, air/moisture stable and readily available, which have been grown into a preferred method when metal-free products are of primary concern (*e.g.* biomedical and microelectronic applications).[52–54] To make dual-initiating LPs truly green/sustainable and user-friendly polymerization catalysts for multiblock copolymers, it is highly desirable to develop metal-free LAs and commercially available dual-initiating LBs. Recently, we have developed a thermally-stable and air/moisture-tolerant organic LP catalyst consisting of tris(2,4-

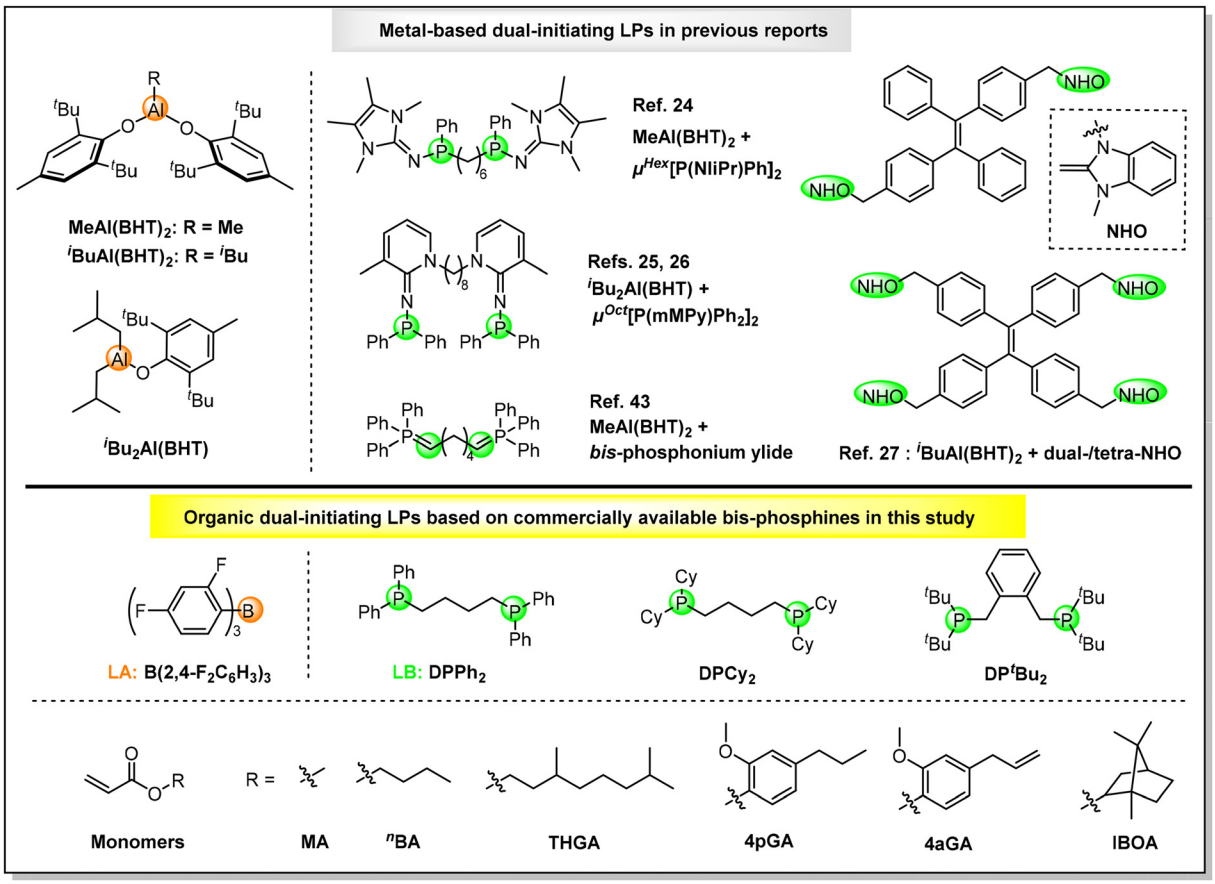

Scheme 1 Structures of metal-based dual-initiating LPs in previous reports (top) and organic dual-initiating LPs and monomers investigated in this study (bottom).

difluorophenyl)borane LA [$B(2,4\text{-}F_2C_6H_3)_3$, Scheme 1, bottom] and triisobutylphosphine (P^iBu_3) LB, which enabled the first efficient and living LPPs of acrylates at ambient and high temperatures (25–80 °C).[39] Herein, commercially available bisphosphines, including 1,4-bis(diphenylphosphino)butane ($DPPh_2$), 1,4-bis(dicyclohexylphosphino)butane ($DPCy_2$), and 1,2-bis[(di-*tert*-butylphosphino)methyl]benzene (DP^tBu_2) (Scheme 1, bottom), have been utilized as LBs in this study. In combination with $B(2,4\text{-}F_2C_6H_3)_3$ LA, organic dual-initiating LPs have been constructed for the first time. Investigations into the polymerization behaviors reveal that $B(2,4\text{-}F_2C_6H_3)_3$/$DP^tBu_2$ is a new robust dual-initiating organic FLP which can mediate efficient and living LPPs of (bio)acrylates, completely chemoselective LPP of divinyl acrylic monomer, and also enable the convenient synthesis of metal-free all-acrylic multiblock copolymers.

Experimental

Materials

All syntheses and manipulations of air- and moisture-sensitive materials were carried out in flamed Schlenk-type glassware on a dual-manifold Schlenk line or in an argon-filled glovebox. HPLC-grade organic solvents were first sparged extensively with nitrogen during the filling of 20 L solvent reservoirs and then dried by passage through activated alumina [for dichloromethane (DCM) and tetrahydrofuran (THF)] followed by passage through Q-5 supported copper catalyst stainless steel columns [for toluene (TOL) and hexane]. Methyl acrylate (MA) and *n*-butyl acrylate (^{n}BA) were purchased from TCI Chemical Co., which were dried over CaH_2 overnight followed by vacuum distillation. Further purification of acrylate monomers involved titration with tri(*n*-octyl)aluminum (Sigma-Aldrich Co.) to a yellow end point, followed by distillation under reduced pressure. Isobornyl acrylate (IBOA) was purchased from TCI Chemical Co., while tetrahydrogeraniol acrylate (THGA), 4-propylguaiacol acrylate (4pGA), and 4-allylguaiacol acrylate (4aGA) were synthesized according to a literature procedure.[59] The obtained four biomass-derived acrylate monomers were dissolved in toluene, dried over CaH_2 overnight, and then filtered in an argon-filled glovebox. The concentrations of these monomers were determined by quantitative ^{1}H NMR spectra. All purified monomers were stored in brown bottles inside a glovebox freezer at −30 °C for further use. 1,4-Bis(diphenylphosphino)butane ($DPPh_2$), 1,2-bis[(di-*tert*-butylphosphino)methyl]benzene (DP^tBu_2), and 1,4-bis(dicyclohexylphosphino)butane ($DPCy_2$) were purchased from Sigma-Aldrich, which were dissolved in toluene and dried over CaH_2 overnight and then filtered in an argon-filled glovebox. The solvent was removed under vacuum, and the residue was dried for 12 h under vacuum. The dried bis-phosphines were stored in brown bottles inside a glovebox freezer at −30 °C for further use. $B(2,4\text{-}F_2C_6H_3)_3$ was synthesized according to a literature procedure.[39]

Stoichiometric reaction of $B(2,4\text{-}F_2C_6H_3)_3$ with bis-phosphines

In a typical procedure, a Teflon-valve-sealed J. Young-type NMR tube was charged with $B(2,4\text{-}F_2C_6H_3)_3$ (35.0 mg, 0.1 mmol) in the glovebox. A solution of bis-phosphine (0.05 mmol) in 0.50 mL of benzene-d_6 or toluene-d_8 was added to the above NMR tube *via* a pipette at RT, and the resulting mixture was then taken out of the glovebox for NMR analysis.

General polymerization procedures

Polymerizations were performed in 20 mL glass reactors inside the glovebox at room temperature (RT). A predetermined amount of LA was first dissolved in a predetermined amount of monomer and solvent inside a glovebox. The mixture was stirred for 10 minutes, and then the polymerization was started by rapid addition of a predetermined amount of Lewis base LB in the solvent *via* a gastight syringe to the above mixture under vigorous stirring. After the measured time interval, a 0.2 mL aliquot was taken from the reaction mixture *via* a syringe and quickly quenched into a 2 mL septum-sealed vial containing 0.4 mL of "wet" $CDCl_3$ mixed with 250 ppm of benzoic acid; the quenched aliquots were later analyzed by ^{1}H NMR spectroscopy to obtain the percent monomer conversion data. After a desired period of time, the polymerization was immediately quenched by the addition of 5 mL of methanol acidified with HCl (5%). The quenched mixture was precipitated into a 100 mL mixed solvent of water and methanol ($V_{water}/V_{methanol}$ = 1/5), filtered and dried in a vacuum oven at 80 °C to a constant weight.

Polymer characterization

NMR spectra were recorded on a Varian 400 MHz spectrometer. Chemical shifts for ^{1}H NMR and ^{13}C NMR spectra were referenced to internal solvent resonances and were reported as parts per million relative to $SiMe_4$. Polymer number average molecular weight (M_n) and molecular weight distributions ($Đ$ = M_w/M_n) were measured by gel permeation chromatography (GPC) analyses carried out at 40 °C and a flow rate of 1.0 mL min^{-1}, with DMF containing a small amount of LiBr (20 mmol L^{-1}) or THF as the eluent on a Waters E2695 GPC instrument equipped with a Wyatt OPTILAB® T-Rex refractive-index detector, a Wyatt DAWN HELEOS II multi (18)-angle light scattering detector, one Agilent Plgel 5 μm guard column, and two Agilent Plgel 5 μm Mixed-C columns (Polymer Laboratories; linear range of MW = 200–2 000 000). Glass-transition temperatures (T_gs) were measured by differential scanning calorimetry (DSC) on a DSC Q2500, TA Instruments. All T_g values were obtained from the second scan after the thermal history was removed from the first scan. The first heating rate was 10 °C min^{-1}, while the cooling rate was 10 °C min^{-1} and the second heating rate was 5 °C min^{-1}. The onset decomposition temperatures (T_d, defined at 5% weight loss) of the polymers were measured by thermal gravimetric analysis (TGA) on a TGA550, TA Instruments. Polymer samples were heated from ambient temperatures to 700 °C at a rate of 20 °C min^{-1}.

The isolated low molecular weight samples were analyzed by matrix assisted laser desorption/ionization time-of-flight

mass spectroscopy (MALDI–TOF MS); the experiment was performed on a Bruker Reflex II mass spectrometer operated in positive ion, reflector mode using a Nd:YAG laser at 355 nm and 25 kV accelerating voltage. A thin layer of a 1% NaI solution was first deposited on the target plate, followed by 0.6 μl of both the sample and matrix (dithranol, 20 mg mL^{-1} in methanol, 10% AAC). External calibration was done using a peptide calibration mixture (4 to 6 peptides) on a spot adjacent to the sample.

Results and discussion

Investigations into the interaction between bis-phosphine and $B(2,4\text{-}F_2C_6H_3)_3$

Considering that the interaction between LA and LB has a significant influence on polymerization activity and initiation efficiency (I^*), the interactions between $B(2,4\text{-}F_2C_6H_3)_3$ and three bis-phosphines were first investigated in our initial study. As shown in Fig. 1A–D and S1, S2 and S4,† the stoichiometric NMR reactions clearly reveal that $DPPh_2$ and $DPCy_2$ form CLAs with $B(2,4\text{-}F_2C_6H_3)_3$, as evidenced by the notable shifts of chemical resonances after the reactions. For example, the chemical resonances of free bis-phosphines ($DPPh_2$: −16.42 ppm, $DPCy_2$: −6.10 ppm) in ^{31}P NMR spectra shift to the downfield [$DPPh_2$ → $B(2,4\text{-}F_2C_6H_3)_3$: 8.07 ppm, $DPCy_2$ → $B(2,4\text{-}F_2C_6H_3)_3$: 3.12 ppm] after the reactions while the shift of the chemical resonances of the $B(2,4\text{-}F_2C_6H_3)_3$ moiety in CLAs can also be observed in ^{19}F NMR spectra [$B(2,4\text{-}F_2C_6H_3)_3$: −94.45, −102.66 ppm; $DPPh_2$ → $B(2,4\text{-}F_2C_6H_3)_3$: −89.92, −112.50 ppm; $DPCy_2$ → $B(2,4\text{-}F_2C_6H_3)_3$: −88.93, −112.73 ppm]. In sharp contrast, in the stoichiometric NMR reaction of $B(2,4\text{-}F_2C_6H_3)_3$ and DP^tBu_2 (Figs. 1E, F and S3, S4†), there were no detectable changes of chemical resonances in ^1H, ^{11}B, ^{31}P, and ^{19}F NMR spectra before and after mixing $B(2,4\text{-}F_2C_6H_3)_3$ and DP^tBu_2, indicating that $DP^tBu_2/B(2,4\text{-}F_2C_6H_3)_3$ is a non-interacting FLP.

Polymerization characteristics of methyl acrylate catalyzed by dual-initiating organic LPs

The above three dual-initiating organic LPs were first employed as the catalysts for the polymerizations of methyl acrylate (MA). With a $[MA]_0:[LA]_0:[LB]_0$ ratio of 200 : 4 : 1, both $DPPh_2$ → $B(2,4\text{-}F_2C_6H_3)_3$ and $DPCy_2$ → $B(2,4\text{-}F_2C_6H_3)_3$ CLAs showed a high degree of control over the polymerizations at room temperature (RT), which afforded PMAs with extremely narrow dispersities ($Đ$ = 1.01) and gave rise to high I^* values of 85.0–86.4% (Table 1, runs 1 and 2). It is interesting that these dual-initiating CLAs can achieve high I^*s in this study, since LPPs by CLA catalysts in previous reports[8–10,28] generally led to low to moderate I^*s because of the irreversible formation of CLAs that is difficult to release free LBs and LAs for initiating polymerization. Such results reveal that both $DPPh_2$ → $B(2,4\text{-}F_2C_6H_3)_3$ and $DPCy_2$ → $B(2,4\text{-}F_2C_6H_3)_3$ CLAs can readily dissociate into FLPs in the presence of a monomer to provide sufficient orthogonal reactivity for fast and efficient initiation. The relatively weak Lewis acidity of $B(2,4\text{-}F_2C_6H_3)_3$,[39] in comparison with commonly used LAs [*e.g.* $B(C_6F_5)_3$, $Al(C_6F_5)_3$, and $MeAl(BHT)_2$], should be responsible for weak LA–LB interactions and thereby facile dissociation. However, in contrast to the corresponding mono-initiating PPh_3 → $B(2,4\text{-}F_2C_6H_3)_3$ and PCy_3 → $B(2,4\text{-}F_2C_6H_3)_3$ CLAs (90–240 min, Conv. >99%, Table 1, runs 3 and 4), these dual-initiating CLAs exhibited much lower polymerization activity, which required 1080–1440 min to consume all MA monomers. A slow propagation process is speculated to be the main reason, which might be caused by the increase of steric hindrance generated from the other propagation site that hampers the activation and conjugate addition. When switching from $DPPh_2$ and $DPCy_2$ with a flexible $-(CH_2)_4-$ linkage between two phosphine moieties to rigid aryl-linked DP^tBu_2, the activity in $DP^tBu_2/B(2,4\text{-}F_2C_6H_3)_3$ FLP-mediated polymerization was significantly enhanced where quantitative monomer conversion was accomplished within 120 min (Table 1, run 5). More importantly, a high degree of control over the polymerization was well maintained, which afforded a PMA with a very low $Đ$ of 1.02 at a high I^* value of 90.2%.

To verify the living nature of $DP^tBu_2/B(2,4\text{-}F_2C_6H_3)_3$ FLP-mediated polymerization, a series of experiments were performed as follows. First, as shown in Fig. 2A, when gradually increasing the ratio of $[MA]_0:[B(2,4\text{-}F_2C_6H_3)_3]_0:[DP^tBu_2]_0$ from 200 : 4 : 1 to 1200 : 4 : 1, a linear increase of the M_ns of PMAs can be observed with predictable M_n values (I^* = 90.2–101.0%) and very low dispersities ($Đ$ = 1.01–1.03) (Table 1, runs 5–8). Noteworthily, even though a large excess of 1200 equivalents of MA were employed, quantitative monomer conversion can also be accomplished within a desirable polymerization time (420 min, Table 1, run 8), producing a PMA with a high M_n of 101.7 kg mol^{-1} and an extremely low $Đ$ of 1.01. Second, keeping $[MA]_0:[B(2,4\text{-}F_2C_6H_3)_3]_0:[DP^tBu_2]_0$ at a fixed ratio of 400 : 4 : 1, the M_n of PMA increases linearly with an increase of monomer conversion, while extremely low $Đ$ values (1.03–1.08) are maintained (Fig. 2B). GPC curves of these samples gradually shift to the higher molecular-weight (MW) region with the increase of the monomer-to-initiator ratio and monomer conversion (Fig. 2C and D) and all show very narrow and unimodal distributions. Third, after the first batch of MA (200 equiv.) was completely converted into PMA, the resulting unquenched system was held at RT for 1 h and then was able to repolymerize immediately once another batch of MA (200 equiv.) was added. The resultant sample showed a narrow and unimodal GPC curve without a detectable low-MW tail (Fig. 2E), and its M_n (34.4 kg mol^{-1}, $Đ$ = 1.02, I^* = 101.1%) was very close to that of the PMA (M_n = 35.1 kg mol^{-1}, $Đ$ = 1.03, I^* = 99.7%) produced by the polymerization at a $[MA]_0/[B(2,4\text{-}F_2C_6H_3)_3]_0/[DP^tBu_2]_0$ ratio of 400 : 4 : 1, clearly demonstrating the successful chain extension. Based on the above three key pieces of evidence, the living characteristic of the $DP^tBu_2/B(2,4\text{-}F_2C_6H_3)_3$ FLP-mediated polymerization of MA has been unequivocally established.

Matrix-assisted laser desorption/ionization time-of-flight mass spectroscopy (MALDI-TOF MS) analysis of low-MW PMA

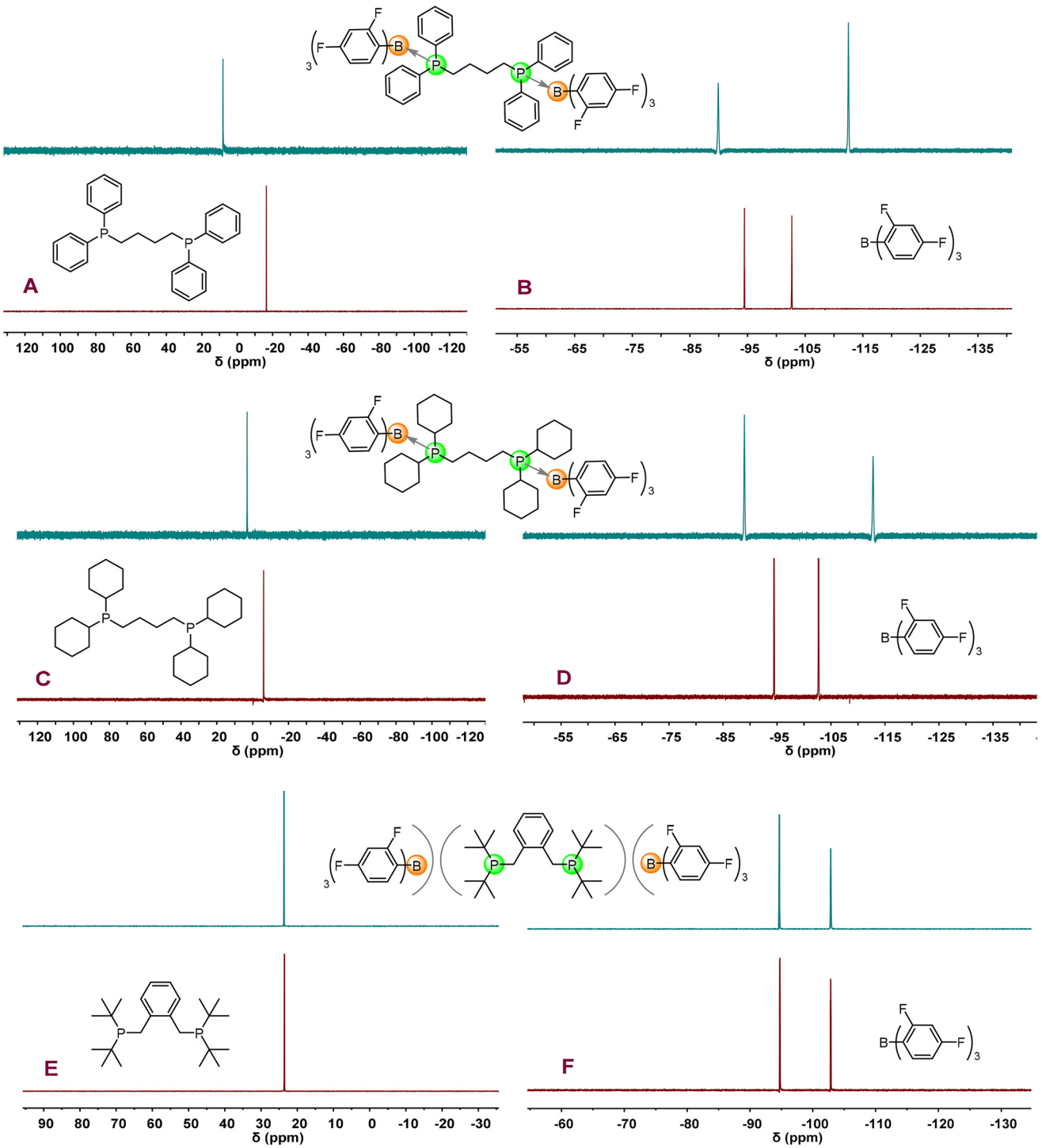

Fig. 1 ^{31}P NMR spectra of $DPPh_2$ → $B(2,4\text{-}F_2C_6H_3)_3$ CLA, $DPCy_2$ → $B(2,4\text{-}F_2C_6H_3)_3$ CLA, $DP^tBu_2/B(2,4\text{-}F_2C_6H_3)_3$ FLP, and their corresponding bisphosphines (A, C and E), as well as the ^{19}F NMR spectra of the above LPs and $B(2,4\text{-}F_2C_6H_3)_3$ (B, D and F) (A–D: toluene-d_8; E and F: benzene-d_6).

was also performed. As shown in Fig. 3, only one set of molecular ion peaks was observed, corresponding to one type of polymer chains starting with the –(^{t}Bu)PCH$_2$ArCH$_2$P(^{t}Bu)– moiety formed by dual initiation from both phosphine sites of DP^tBu_2 LB and the subsequent elimination of two *tert*-butyl groups from –(^{t}Bu)$_2$P$^+$CH$_2$ArCH$_2$P$^+$(^{t}Bu)$_2$– during the MALDI-TOF MS measurement. After the quenching process, two H-terminated chain ends were generated. This result further confirms that $DP^tBu_2/B(2,4\text{-}F_2C_6H_3)_3$ FLP-mediated polymerization proceeds in a living manner without any backbiting termination and chain transfer events and, more importantly, clearly demonstrates an exclusive dual initiation

Table 1 Results of acrylate polymerizations by B(2,4-$F_2C_6H_3$)$_3$-based dual-initiating LP catalysts[a]

Run	LB	M.	$[M.]_0 : [LA]_0 : [LB]_0$	$[M.]_0$ (mol L^{-1})	Time (min)	Conv.[b] (%)	M_n[c] (kg mol^{-1})	$Đ$[c]	I^*[d] (%)
1	$DPPh_2$	MA	200 : 4 : 1	1.0	1440	>99	20.4	1.01	86.4
2	$DPCy_2$	MA	200 : 4 : 1	1.0	1080	>99	20.8	1.01	85.0
3[e]	PPh_3	MA	100 : 2 : 1	1.0	240	>99	40.7	1.06	21.7
4[e]	PCy_3	MA	100 : 2 : 1	1.0	90	>99	9.30	1.02	95.5
5	DP^tBu_2	MA	200 : 4 : 1	1.0	120	>99	19.5	1.02	90.2
6	DP^tBu_2	MA	400 : 4 : 1	1.5	210	>99	35.1	1.03	99.7
7	DP^tBu_2	MA	800 : 4 : 1	2.0	300	>99	71.4	1.02	97.0
8	DP^tBu_2	MA	1200 : 4 : 1	2.5	420	>99	101.7	1.01	101.0
9	DP^tBu_2	^{n}BA	200 : 4 : 1	1.0	30	>99	30.2	1.09	86.1
10	DP^tBu_2	^{n}BA	1200 : 4 : 1	2.5	120	>99	180.3	1.01	85.4
11	DP^tBu_2	4pGA	200 : 4 : 1	1.0	40	>99	46.9	1.07	96.1
12	DP^tBu_2	4pGA	800 : 4 : 1	1.5	150	>99	217.7	1.17	81.0
13	DP^tBu_2	4aGA	200 : 4 : 1	1.0	40	>99	44.8	1.08	98.2
14	DP^tBu_2	4aGA	800 : 4 : 1	1.5	150	>99	216.2	1.15	80.1
15	DP^tBu_2	THGA	200 : 4 : 1	1.0	50	>99	43.4[f]	1.08	98.5
16	DP^tBu_2	THGA	800 : 4 : 1	1.5	240	>99	175.1[f]	1.21	97.1
17	DP^tBu_2	IBOA	200 : 4 : 1	1.0	120	>99	52.9[f]	1.12	80.0
18	DP^tBu_2	IBOA	800 : 4 : 1	1.5	300	>99	170.0[f]	1.13	98.1

[a] The polymerizations were carried out by premixing LA and the monomer (M.) first followed by adding LB unless otherwise noted: LB = 0.01 mmol, Temp. = 25 °C, toluene as the solvent. [b] Monomer conversion measured by ^{1}H NMR spectroscopy. [c] Number-average molecular weight (M_n) and molecular weight distribution ($Đ = M_w/M_n$) determined by GPC at 40 °C in DMF coupled with a multi(18)-angle light scattering detector and a refractive index detector. [d] Initiation efficiency (I^*)% = M_n(calcd)/M_n(exptl) × 100, where M_n(calcd) = [MW(M.)] × ($[M.]_0/[LB]_0$) × conversion% + MW(LB) + MW(end groups). [e] Initiation efficiency (I^*)% = M_n(calcd)/M_n(exptl) × 100, where M_n(calcd) = [MW(M.)] × ($[M.]_0/[LB]_0$) × conversion% + MW(end groups). [f] THF as the eluent in GPC measurement.

process that facilitates the synthesis of multi-block copolymers.

DP^tBu_2/B(2,4-$F_2C_6H_3$)$_3$ FLP-mediated living polymerizations of (bio)acrylates to all-acrylic multiblock copolymers

Having established the DP^tBu_2/B(2,4-$F_2C_6H_3$)$_3$ FLP as the best dual-initiating catalyst for efficient and living polymerization of MA, the scope of monomers was further explored. Again, the polymerization of *n*-butyl acrylate (^{n}BA) by the DP^tBu_2/B(2,4-$F_2C_6H_3$)$_3$ FLP still proceeded in a living manner, affording P^{n}BAs with very low $Đ$s of 1.01–1.09 at high I^* values of 85.4–86.1% (Table 1, runs 9 and 10). It is worth noting that this FLP is especially effective for ^{n}BA polymerization, where 1200 equivalents of ^{n}BA were rapidly polymerized within 120 min (Table 1, run 10), which was 3 times faster than MA polymerization under the same conditions (Table 1, run 8).

Besides, bio-based acrylates were also utilized as the monomers, including tetrahydrogeraniol acrylate (THGA), 4-propylguaiacol acrylate (4pGA), 4-allylguaiacol acrylate (4aGA) and isobornyl acrylate (IBOA) (Scheme 1). Among them, IBOA is commercially available, while THGA, 4pGA, and 4aGA can be synthesized *via* a one-step reaction of acryloyl chloride and biomass-derived alcohols with high yields (71.2–82.1%) (Fig. S5–S10†). Presumably due to the bulkier side groups of these monomers, their polymerizations by the DP^tBu_2/B(2,4-$F_2C_6H_3$)$_3$ FLP were relatively slower than ^{n}BA (Table 1, runs 11–18). At a low monomer loading (200 : 4 : 1), living polymerizations of these monomers can also be achieved. High to quantitative I^* values (80.0–98.5%) and narrow unimodal distributions ($Đ$ = 1.07–1.21) were well-maintained. However, in the cases of high-monomer-loading LPPs (800 : 4 : 1), a significant increase of the viscosity of the polymerization mixture was observed at the late stage of polymerization. Therefore, decreasing the monomer concentration from 2.0 to 1.5 M was necessary to relieve unfavorable monomer diffusion at the late stage of polymerization. Accordingly, upon the employment of dilute conditions, controlled polymerizations at a high monomer loading can also be achieved, producing high-M_n bio-based polyacrylates (170.0–217.7 kg mol^{-1}) with relatively narrow dispersities ($Đ$s: 1.13–1.21). The structures of these bio-based polyacrylates were fully characterized by NMR spectra (Fig. S11–S18†). Of particular note is the completely chemoselective polymerization of 4aGA rendered by the DP^tBu_2/B(2,4-$F_2C_6H_3$)$_3$ FLP, as evidenced by the complete disappearance of acrylic double bonds at 5.94–6.02, 6.31–6.39, and 6.59–6.63 ppm after the polymerization while the allyl groups at 5.92 and 5.08–5.14 ppm remain unreacted (Fig. 4). As a result, soluble P4aGA without any cross-linking was obtained with pendant double bonds on the side groups, which thus offers great potential in the synthesis of functional or advanced acrylic polymers.

The unique living and dual-initiating nature of organic DP^tBu_2/B(2,4-$F_2C_6H_3$)$_3$ FLP-mediated polymerizations of acrylates thereby enabled the convenient synthesis of metal-free multiblock copolymers *via* sequential monomer addition. Accordingly, besides P^{n}BA-*b*-PMA-*b*-P^{n}BA and bio-based PIBOA-*b*-PTHGA-*b*-PIBOA triblock copolymers, P4pGA-*b*-P^{n}BA-*b*-PMA-*b*-P^{n}BA-*b*-P4pGA pentablock and P4aGA-*b*-P4pGA-*b*-P^{n}BA-*b*-PMA-*b*-P^{n}BA-*b*-P4pGA-*b*-P4aGA heptablock copolymers can also be readily prepared using three and four steps of comonomer additions, respectively. As shown in Fig. 5, even though the unquenched polymerization mixture was held for 30 min

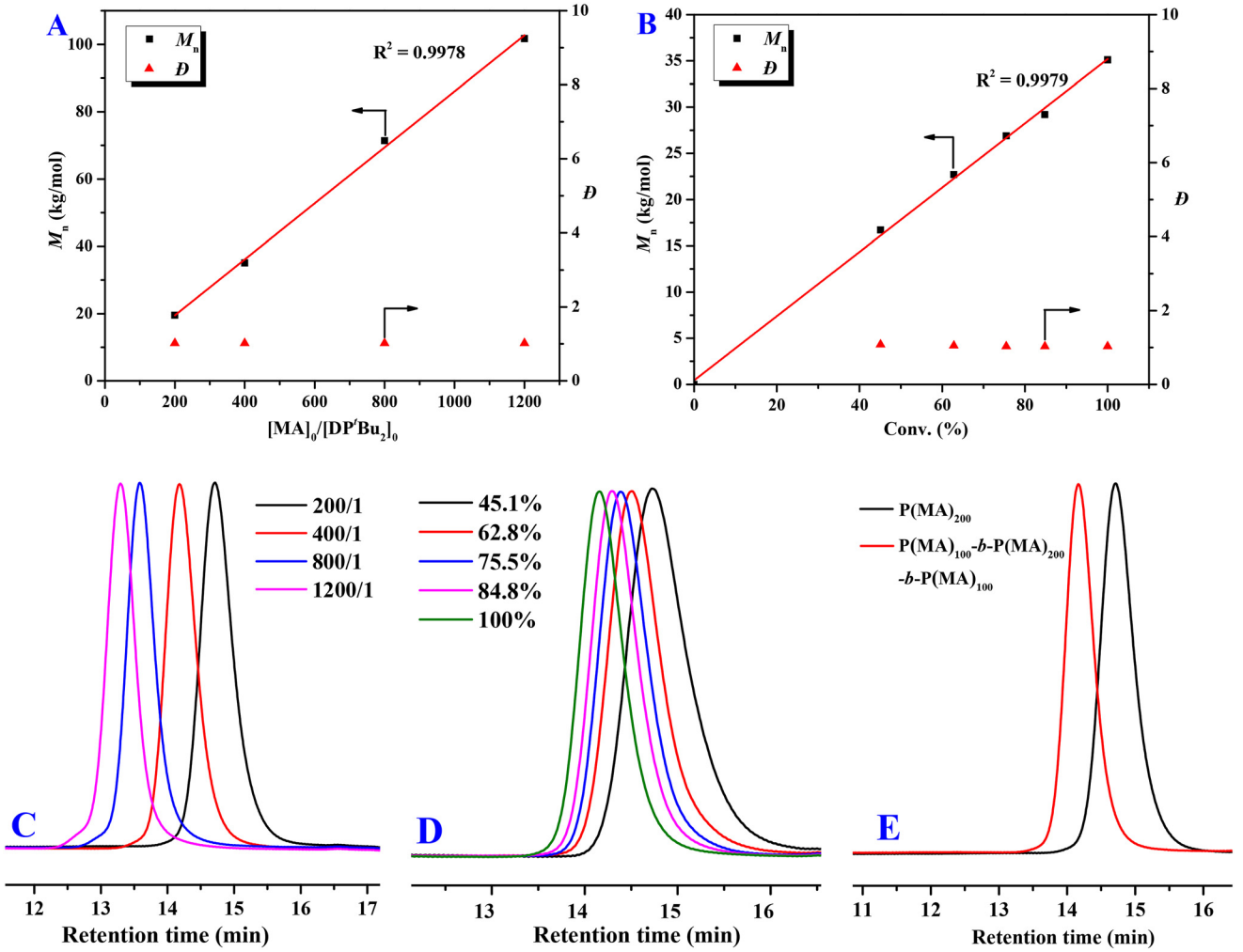

Fig. 2 (A) Plots of M_n and $Đ$ for the PMA *vs.* the $[MA]_0 : [DP^tBu_2]_0$ ratio (Table 1, runs 5–8); (B) plots of M_n and $Đ$ for the PMA *vs.* monomer conversion (%) (Conv. % = 45.1, 62.8, 75.5, 84.8, 100%; M_n = 16.7, 22.7, 26.8, 29.2, 35.1 kg mol^{-1}; $Đ$ = 1.08, 1.05, 1.03, 1.04, 1.03); (C) GPC curves of PMAs produced at different $[MA]_0 : [DP^tBu_2]_0$ ratios (Table 1, runs 5–8); (D) GPC curves of PMAs produced at different monomer conversions ($[MA]_0 : [DP^tBu_2]_0$ = 400 : 1); (E) GPC curves of PMA samples obtained by the chain extension experiment: M_n = 19.5 kg mol^{-1}, $Đ$ = 1.02 (first batch) and M_n = 34.4 kg mol^{-1}, $Đ$ = 1.02 (second batch after 1 h).

before the addition of the next batch of comonomers, GPC curves of the resultant samples maintained very narrow and unimodal distributions without any detectable low-MW tails and gradually shifted to higher MW regions with the increase of block numbers, confirming the livingness/stability of the propagating species that ensures the successful block copolymerizations. It is worth pointing out that there was essentially no effect of comonomer addition order on the polymerization outcome. For example, identical MWs and distributions can be achieved in the block copolymerization of ^{n}BA and MA with different monomer addition orders (P^{n}BA-*b*-PMA-*b*-P^{n}BA: M_n = 40.5 kg mol^{-1}, $Đ$ = 1.03, Fig. 5A; PMA-*b*-P^{n}BA-*b*-PMA: M_n = 38.4 kg mol^{-1}, $Đ$ = 1.09, Fig. S19†).

The thermal properties of these bio-based acrylic homopolymers and all-acrylic multiblock copolymers were examined by differential scanning calorimetry (DSC) and thermal gravimetric analysis (TGA). The second heating scans of DSC curves of bio-based acrylic homopolymers (Fig. 6A) show glass transition temperatures (T_gs) that vary over a large range: PTHGA with flexible side groups exhibits a low T_g of −60.0 °C, while P4pGA (58.6 °C), P4aGA (58.1 °C), and PIBOA (99.1 °C) with rigid side groups possess high T_gs. In the case of multiblock copolymers (Fig. 6B), multi-T_gs corresponding to different blocks can be observed, which demonstrates the microphase separation between these blocks and thus indicates the potential applications of these multiblock copolymers in TPEs and self-assembling nanomaterials. For example, the P4pGA-*b*-P^{n}BA-*b*-PMA-*b*-P^{n}BA-*b*-P4pGA pentablock shows T_g values of −42.0, 20.0, and 56.6 °C, corresponding to P^{n}BA, PMA, and P4pGA blocks, respectively.

As shown in Fig. 6C, TGA analysis reveals that bio-based PTHGA, P4pGA, and P4aGA homopolymers exhibit high thermal stability by showing a sharp, one-step degradation profile with a high onset degradation temperature (T_d, defined

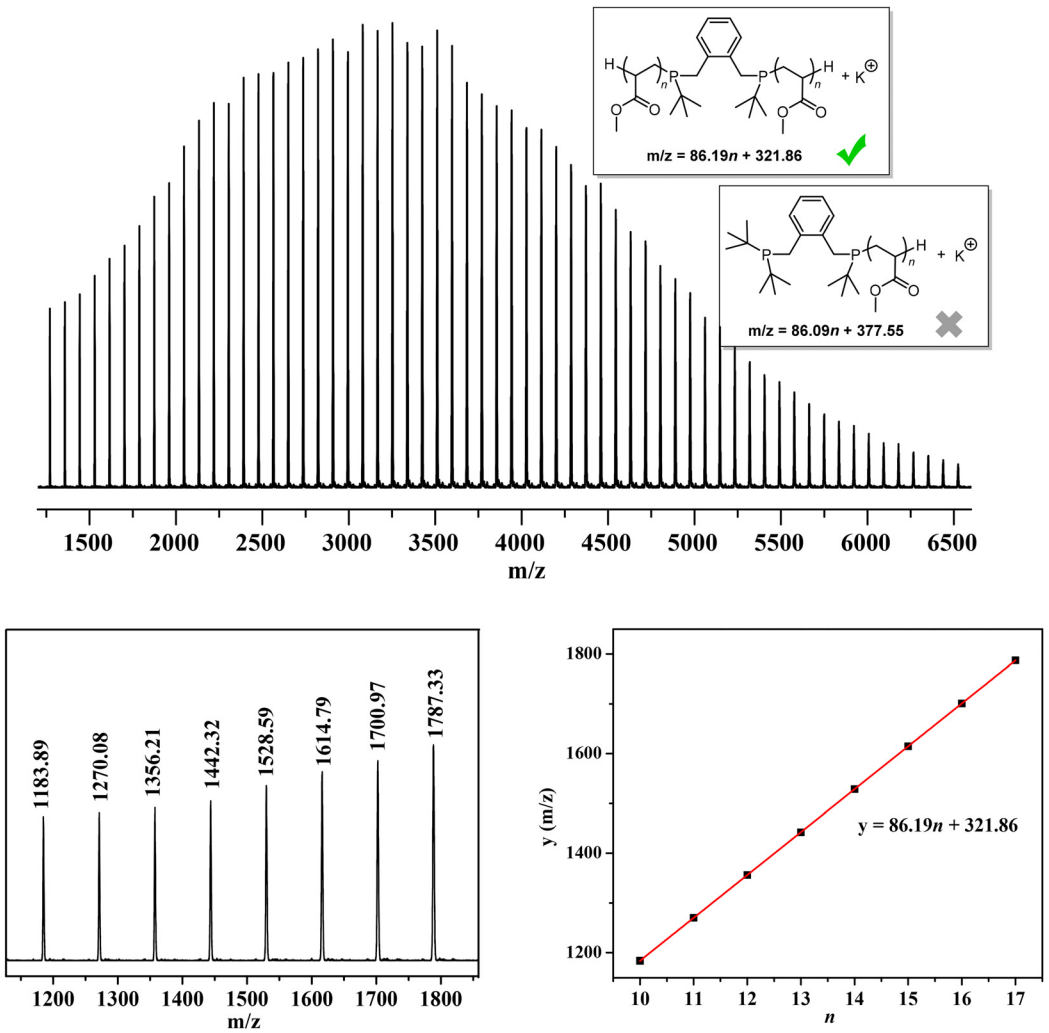

Fig. 3 MALDI-TOF MS spectrum of low-MW PMAs and plots of *m*/*z* values (*y*) *vs*. the number of MS repeat units (*n*) for molecular ion peaks.

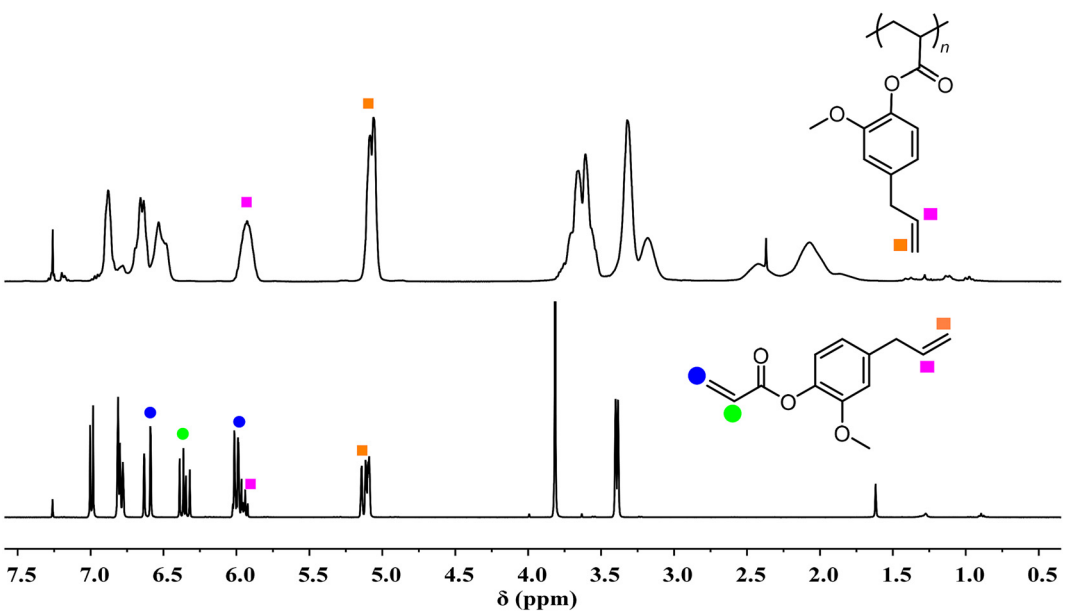

Fig. 4 ^{1}H NMR spectra ($CDCl_3$, RT): (top) P4aGA produced by the DP^{t}Bu$_2$/B(2,4-$F_2C_6H_3$)$_3$ FLP (Table 1, run 13); (bottom) 4aGA monomer.

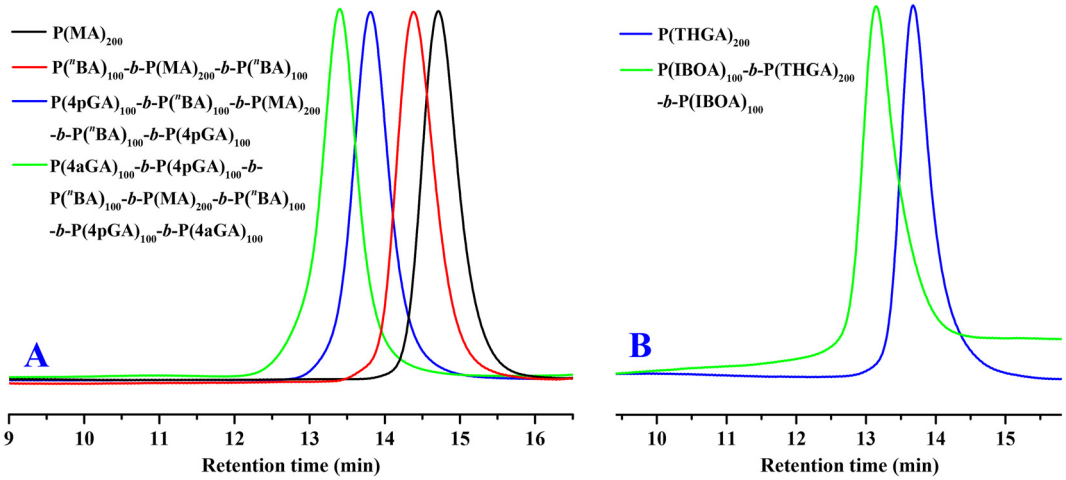

Fig. 5 (A) GPC curves of the PMA homopolymer (M_n = 19.5 kg mol^{-1}, $Đ$ = 1.02), the P^{n}BA-*b*-PMA-*b*-P^{n}BA triblock (M_n = 40.5 kg mol^{-1}, $Đ$ = 1.03), the P4pGA-*b*-P^{n}BA-*b*-PMA-*b*-P^{n}BA-*b*-P4pGA pentablock (M_n = 102.3 kg mol^{-1}, $Đ$ = 1.05), and P4aGA-*b*-P4pGA-*b*-P^{n}BA-*b*-PMA-*b*-P^{n}BA-*b*-P4pGA-*b*-P4aGA (M_n = 158.5 kg mol^{-1}, $Đ$ = 1.07) heptablock copolymers; (B) GPC curves of the PTHGA homopolymer (M_n = 43.4 kg mol^{-1}, $Đ$ = 1.08) and the PIBOA-*b*-PTHGA-*b*-PIBOA triblock copolymer (M_n = 78.4 kg mol^{-1}, $Đ$ = 1.18).

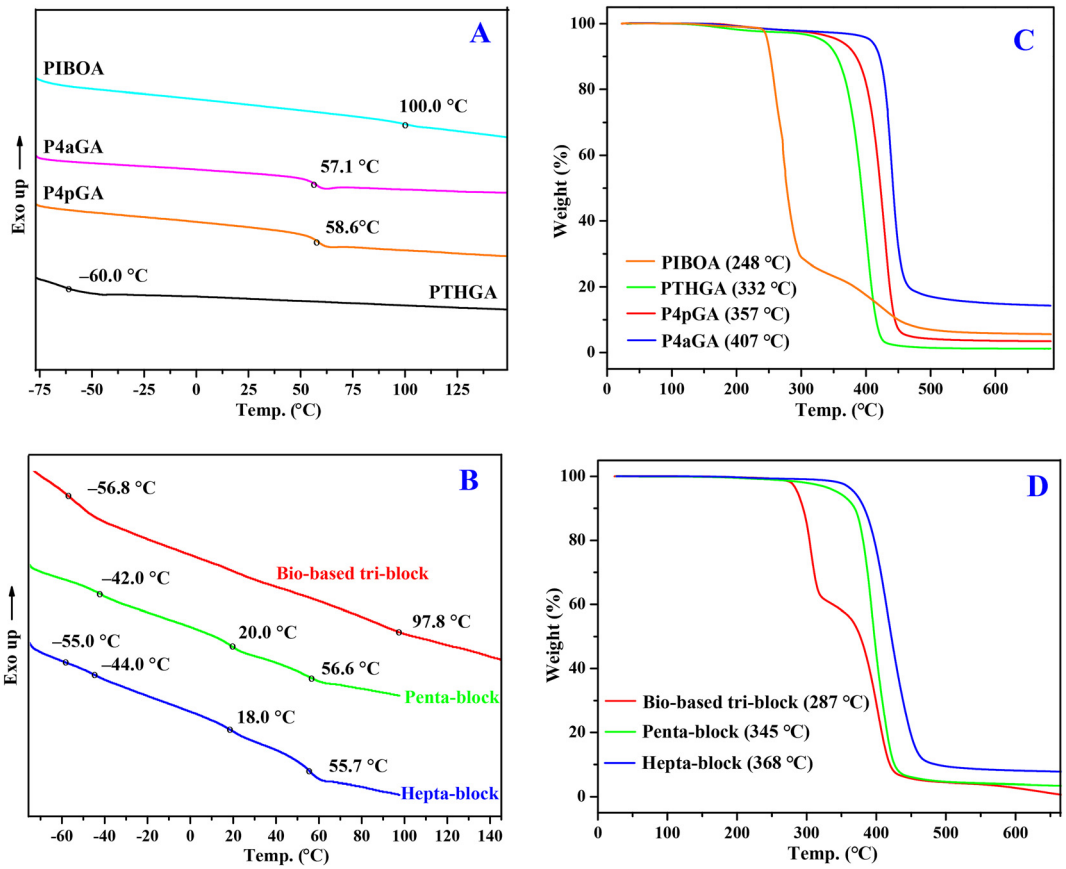

Fig. 6 Overlays of the second heating scan DSC curves (A) and TGA curves (C) of PTHGA, P4pGA, P4aGA, and PIBOA homopolymers as well as overlays of the second heating scan DSC curves (B) and TGA curves (D) of the PIBOA-*b*-THGA-*b*-PIBOA triblock, the P4pGA-*b*-P^{n}BA-*b*-PMA-*b*-P^{n}BA-*b*-P4pGA pentablock, and P4aGA-*b*-P4pGA-*b*-P^{n}BA-*b*-PMA-*b*-P^{n}BA-*b*-P4pGA-*b*-P4aGA heptablock copolymers.

by the temperatures of 5% weight loss) ranging from 332 to 407 °C. It should be pointed out that noticeable carbonaceous material remained after the TGA measurement of P4aGA (*ca.* 15% mass), which should be attributed to the formation of a cross-linked network structure during the heating caused by the allyl group. In contrast, the thermal stability of PIBOA is relatively low with a T_d of 248 °C, presumably due to the good leaving ability of the bulky side group. Moreover, a two-step degradation profile is observed for PIBOA, including the leaving of side groups and subsequently thermal degradation of backbones. In the case of multiblock copolymers (Fig. 6D), their T_d values are somewhere between high-T_d and low-T_d blocks. Taking the bio-based PIBOA-*b*-PTHGA-*b*-PIBOA triblock copolymer as an example, its T_d value (287 °C) is higher than the corresponding PIBOA homopolymer (248 °C) but lower than the PTHGA homopolymer (332 °C). Except for the bio-based triblock copolymer that exhibits a two-step degradation profile, both penta- and heptablock copolymers show a one-step degradation profile, indicating a similar thermal degradation behavior between blocks.

Conclusions

In summary, organic dual-initiating LP catalysts consisting of $B(2,4\text{-}F_2C_6H_3)_3$ LA and three commercially available bisphosphine LBs have been reported for the first time in this study. All these three LP catalysts exhibit high control over the polymerizations of MA but show different polymerization activities: $DPPh_2$ → $B(2,4\text{-}F_2C_6H_3)_3$ and $DPCy_2$ → $B(2,4\text{-}F_2C_6H_3)_3$ CLAs based on bisphosphines with flexible $-(CH_2)_4-$ linkages have relatively low polymerization activity, featured with fast initiation but slow propagation, while the rigid aryl-linked $DP^tBu_2/B(2,4\text{-}F_2C_6H_3)_3$ FLP can mediate efficient polymerizations with significantly enhanced activity. The living characteristic of $DP^tBu_2/B(2,4\text{-}F_2C_6H_3)_3$-mediated LPPs of MA has been unequivocally established by the linear increase of polymer M_n *vs.* monomer conversion and the monomer-to-initiator ratio with predictable polymer M_ns (up to 101.7 kg mol^{-1}), extremely low $Đ$s (1.01–1.03), and high to near quantitative I^*s (90.2–101.0%) as well as successful chain extension. Besides commonly used MA and ^{n}BA, the (chemoselective) polymerizations of bio-based acrylates (THGA, 4pGA, 4aGA and IBOA) by the $DP^tBu_2/B(2,4\text{-}F_2C_6H_3)_3$ FLP also proceed in a living manner. Accordingly, multiblock copolymers (up to hepta blocks) with well-defined structures can be readily prepared *via* sequential monomer addition. The notable features of the $DP^tBu_2/B(2,4\text{-}F_2C_6H_3)_3$ FLP, including the utilization of organic LA and commercially available LB as well as its living and dual-initiating nature, thus successfully establish it as a green/sustainable and user-friendly polymerization catalyst for the convenient synthesis of metal-free all-acrylic multiblock copolymers. The existence of microphase separation as evidenced by multi-T_gs indicates the potential applications of these multiblock copolymers in TPEs and self-assembling nanomaterials, which are currently in progress.

Data availability

The data supporting this article can be found in the tables and figures of the manuscript and its ESI.†

Conflicts of interest

There are no conflicts to declare.

Acknowledgements

This work was supported by the National Key R&D Program of China (2021YFA1501700), the National Natural Science Foundation of China (Grant No. 22471286), the Science and Technology Commission of Shanghai Municipality (Grant No. 22ZR1481900 and 23XD1424600), the Strategic Priority Research Program of the Chinese Academy of Sciences (Grant No. XDB0610000), and the CAS Project for Young Scientists in Basic Research (Grant No. YSBR-094).

References

1 M. Hong, J. Chen and E. Y.-X. Chen, *Chem. Rev.*, 2018, **118**, 10551–10616.
2 M. Hong, *Frustrated Lewis Pairs, Molecular Catalysis 2*, Springer Cham, Switzerland, 2021, pp. 283–317.
3 M. L. McGraw and E. Y.-X. Chen, *Macromolecules*, 2020, **53**, 6102–6122.
4 W. Zhao, J. He and Y. Zhang, *Sci. Bull.*, 2019, **64**, 1830–1840.
5 W. Zhao, J. He and Y. Zhang, *Sci. China: Chem.*, 2023, **66**, 2256–2266.
6 G. C. Welch, R. R. S. Juan, J. D. Masuda and D. W. Stephan, *Science*, 2006, **314**, 1124–1126.
7 D. W. Stephan, *Science*, 2016, **354**, aaf7229.
8 Y. Zhang, G. M. Miyake and E. Y.-X. Chen, *Angew. Chem., Int. Ed.*, 2010, **49**, 10158–10162.
9 T. Xu and E. Y.-X. Chen, *J. Am. Chem. Soc.*, 2014, **136**, 1774–1777.
10 J. He, Y. Zhang, L. Falivene, L. Caporaso, L. Cavallo and E. Y.-X. Chen, *Macromolecules*, 2014, **47**, 7765–7774.
11 M. L. McGraw, R. W. Clarke and E. Y.-X. Chen, *J. Am. Chem. Soc.*, 2020, **142**, 5969–5973.
12 L. T. Reilly, M. L. McGraw, F. D. Eckstrom, R. W. Clarke, K. A. Franklin, E. R. Chokkapu, L. Cavallo, L. Falivene and E. Y.-X. Chen, *J. Am. Chem. Soc.*, 2022, **144**, 23572–22358.
13 M. L. McGraw, R. W. Clarke and E. Y.-X. Chen, *J. Am. Chem. Soc.*, 2021, **143**, 3318–3322.
14 R. W. Clarke, M. R. Caputo, L. P. Fonseca, M. L. McGraw, L. T. Reilly, K. A. Franklin, A. J. Müller and E. Y.-X. Chen, *J. Am. Chem. Soc.*, 2024, **146**, 4930–4941.
15 M. McGraw and E. Y.-X. Chen, *ACS Catal.*, 2018, **8**, 9877–9887.

16 Q. Wang, W. Zhao, S. Zhang, J. He, Y. Zhang and E. Y.-X. Chen, *ACS Catal.*, 2018, **8**, 3571–3578.
17 Y. Bai, J. He and Y. Zhang, *Angew. Chem., Int. Ed.*, 2018, **57**, 17230–17234.
18 Y. Bai, H. Wang, J. He and Y. Zhang, *Angew. Chem., Int. Ed.*, 2020, **59**, 11613–11619.
19 W. Zhao, F. Li, C. Li, J. He, Y. Zhang and C. Chen, *Angew. Chem., Int. Ed.*, 2021, **60**, 24306–24311.
20 H. Wang, Q. Wang, J. He and Y. Zhang, *Polym. Chem.*, 2019, **10**, 3597–3603.
21 W. Zhao, Q. Wang, J. He and Y. Zhang, *Polym. Chem.*, 2019, **10**, 4328–4335.
22 Y. Wan, W. Zhao, H. Zhao, M. Zhou, J. He and Y. Zhang, *Macromolecules*, 2023, **56**, 7763–7770.
23 Y. Song, J. He, Y. Zhang, R. A. Gilsdorf and E. Y.-X. Chen, *Nat. Chem.*, 2023, **15**, 366–376.
24 Y. Bai, H. Wang, J. He, Y. Zhang and E. Y.-X. Chen, *Nat. Commun.*, 2021, **12**, 4874.
25 Y. Wan, J. He, Y. Zhang and E. Y.-X. Chen, *Angew. Chem., Int. Ed.*, 2022, **61**, e202114946.
26 Y. Wan, J. He and Y. Zhang, *Angew. Chem., Int. Ed.*, 2023, **62**, e202218248.
27 C. Li, W. Zhao, J. He and Y. Zhang, *Angew. Chem., Int. Ed.*, 2024, **63**, e202401265.
28 Y.-B. Jia, Y.-B. Wang, W.-M. Ren, T. Xu, J. Wang and X.-B. Lu, *Macromolecules*, 2014, **47**, 1966–1972.
29 Y.-B. Jia, W.-M. Ren, S.-J. Liu, T. Xu, Y.-B. Wang and X.-B. Lu, *ACS Macro Lett.*, 2014, **3**, 896–899.
30 P. Zhang, H. Zhou and X.-B. Lu, *Macromolecules*, 2019, **52**, 4520–4525.
31 P. Xu, L. Wu, L. Dong and X. Xu, *Molecules*, 2018, **23**, 360.
32 P. Xu and X. Xu, *ACS Catal.*, 2018, **8**, 198–202.
33 P. Xu, Y. Yao and X. Xu, *Chem. – Eur. J.*, 2017, **23**, 1263–1267.
34 Y. Su, Y. Zhao, H. Zhang, Y. Luo and X. Xu, *Macromolecules*, 2021, **54**, 7724–7731.
35 Y. Zhou, S. Jiang and X. Xu, *Chin. J. Chem.*, 2021, **39**, 149–156.
36 X. Wang and M. Hong, *Macromolecules*, 2020, **53**, 4659–4669.
37 X.-J. Wang and M. Hong, *Angew. Chem., Int. Ed.*, 2020, **59**, 2664–2668.
38 X. Wang, Y. Zhang and M. Hong, *Polym. Chem.*, 2023, **14**, 3286–3293.
39 Z.-H. Zhang, X. Wang, X.-J. Wang, Y. Li and M. Hong, *Macromolecules*, 2021, **54**, 8495–8502.
40 Z.-H. Zhang, X. Wang, B. Weng, Y. Zhang, G. Zhang and M. Hong, *ACS Polym. Au*, 2022, **2**, 266–274.
41 Z. Zhang, X. Wu and M. Hong, *Acta Polym. Sin.*, 2022, **53**, 1150–1160.
42 Z.-K. Chen, W.-C. Zhao, Y.-L. Zhao, C.-L. Liu, L.-Y. Jiang, Y.-T. Zhang and H.-P. Zhu, *Chin. J. Polym. Sci.*, 2024, **42**, 159–167.
43 C. Liu, W. Zhao, L. Li, Z. Chen, Y. Zhao, Y. Zhang and H. Zhu, *Macromolecules*, 2024, **57**, 110–121.
44 M. Weger, R. K. Grötsch, M. G. Knaus, M. M. Giuman, D. C. Mayer, P. J. Altmann, E. Mossou, B. Dittrich, A. Pöthig and B. Rieger, *Angew. Chem., Int. Ed.*, 2019, **58**, 9797–9801.
45 M. G. M. Knaus, M. M. Giuman, A. Pöthig and B. Rieger, *J. Am. Chem. Soc.*, 2016, **138**, 7776–7781.
46 Y. Hosoi, A. Takasu, S. Matsuoka and M. Hayashi, *J. Am. Chem. Soc.*, 2017, **139**, 15005–15012.
47 H. Yato, K. Oto, A. Takasu and M. Higuchi, *RSC Adv.*, 2023, **13**, 13616–13623.
48 R. Akita, M. Horibe, K. Yamamoto and S. Matsuoka, *Macromolecules*, 2024, **57**, 4926–4936.
49 R. Akita and S. Matsuoka, *ACS Macro Lett.*, 2024, **13**, 1272–1278.
50 Y. Naganawa, K. Mori, S. Matsuoka and M. Suzuki, *Polym. J.*, 2024, **56**, 145–151.
51 Z. Wang, X. Zhang, H. Liang, M. Xian and X. Wang, *Polym. Chem.*, 2020, **11**, 5526–5533.
52 J. Chen and E. Y.-X. Chen, *Isr. J. Chem.*, 2015, **55**, 216–225.
53 F. S. Bates, M. A. Hillmyer, T. P. Lodge, C. M. Bates, K. T. Delaney and G. H. Fredrickson, *Science*, 2012, **336**, 434–440.
54 N. G. Engelis, A. Anastasaki, G. Nurumbetov, N. P. Truong, V. Nikolaou, A. Shegiwal, M. R. Whittaker, T. P. Davis and D. M. Haddleton, *Nat. Chem.*, 2017, **9**, 171–178.
55 A. Anastasaki, B. Oschmann, J. Willenbacher, A. Melker, M. H. C. van Son, N. P. Truong, M. W. Schulze, E. H. Discekici, A. J. McGrath, T. P. Davis, C. M. Bates and C. J. Hawker, *Angew. Chem., Int. Ed.*, 2017, **56**, 14483–14487.
56 N. E. Kamber, W. Jeong, R. M. Waymouth, R. C. Pratt, B. G. G. Lohmeijer and J. L. Hedrick, *Chem. Rev.*, 2007, **107**, 5813–5840.
57 S. Naumann and A. P. Dove, *Polym. Chem.*, 2015, **6**, 3185–3200.
58 W. N. Ottou, H. Sardon, D. Mecerreyes, J. Vignolle and D. Taton, *Prog. Polym. Sci.*, 2016, **56**, 64–115.
59 S. Noppalit, A. Simula, N. Ballard, X. Callies, J. M. Asua and L. Billon, *Biomacromolecules*, 2019, **20**, 2241–2251.

